Artifacts in Dual-Energy CT Gout Protocol: A Review of 50 Suspected Cases With an Artifact Identification Guide

Paul Ian Mallinson[1]
Tyler Coupal[2]
Clemens Reisinger[1]
Hong Chou[1]
Peter Loren Munk[1]
Savvas Nicolaou[1]
Hugue Ouellette[1]

OBJECTIVE. The objective of our study was to discover the types and incidence of artifacts in dual-energy CT (DECT) using datasets of 50 consecutive patients who underwent a four-limb DECT protocol for the evaluation of suspected gout. Identification of artifacts and techniques for artifact reduction are discussed.

CONCLUSION. Artifacts commonly occur in DECT performed for gout assessment but are usually readily recognizable. For 90% of the patients in our study who underwent imaging for suspected gout, DECT showed some type of artifact, with nail bed and skin artifacts being the most common.

Keywords: artifact, artifact reduction, dual-energy CT, gout, urate

DOI:10.2214/AJR.13.11396

Received June 3, 2013; accepted after revision October 8, 2013.

[1]Department of Radiology, Vancouver General Hospital and University of British Columbia, 899 W 12th Ave, Vancouver, BC V5Z 1M9, Canada. Address correspondence to P. I. Mallinson (paul.mallinson@vch.ca).

[2]De Groote School of Medicine, McMaster University, Hamilton, ON, Canada.

WEB
This is a web exclusive article.

AJR 2014; 203:W103–W109

0361–803X/14/2031–W103

Gout is an inflammatory arthropathy that is characterized by acute attacks of joint pain and swelling in the early stages and by joint destruction, renal disease, and possibly cardiac disease in the late stages [1, 2]. Classically diagnosis has been clinical, with the clinical findings being supported by joint aspiration and microscopy results showing the characteristic negatively birefringent crystals [3]. Aspiration is considered the reference standard but is invasive, with the risk of potential complications [4]. The clinical diagnosis of gout can be difficult because of coexistent and mimicking conditions such as osteoarthritis, rheumatoid arthritis, and infection. DECT offers a rapid, noninvasive, and sensitive method of urate detection that can negate the need for invasive procedures and can detect gout in the preclinical stages [5–7]. Detection of gout in the preclinical stages allows early diagnosis and treatment, and treatment, in turn, has the potential to reduce the chance of long-term musculoskeletal, cardiac, and renal complications.

A DECT scanner works by simultaneously scanning the subject at two different energy levels using two x-ray sources and corresponding detector arrays within the same gantry. For many tissues, the beam attenuation does not vary significantly with the energy level range used for diagnostic CT. However, in some substances, including urate and calcium, the difference in photoelectric effect between the two levels creates a measureable attenuation difference, and this difference in attenuation, in turn, enables urate detection and separation from adjacent calcium and soft tissues. Urate and calcium can then be coded different colors and fused over the regular gray-scale CT images to produce a highly accurate map of the urate within the body: Sensitivities of 78–100% and specificities of 89–100% have been reported [7–9].

However, not all material color coded as urate on DECT images corresponds to likely or actual locations of urate deposition. Reported sites of such artifact include the skin, nose, calluses, nail bed, tissues around arthroplasties, and the flexor and peroneal tendons [8, 10, 11]. These artifacts have the potential to lead to a false-positive result if not recognized by the reporting radiologist.

DECT is a valuable new tool for the diagnosis of gout. Our aim in this study was to evaluate the incidence of the various types of artifacts in DECT performed to evaluate for suspected gout, provide a guide for the reporting radiologist to use to identify these artifacts, and discuss artifact-reduction techniques.

Materials and Methods

This study was approved by the research ethics board and patient consent was obtained to review patient records and images. There was no industry or commercial financial support provided for this study.

In our institution, a four-limb DECT protocol is performed of patients with suspected gout. This gout protocol comprises four sets of paired imag-

TABLE 1: Settings for Upper and Lower Limb Dual-Energy CT (DECT) Gout Protocol

Parameter	Body Part							
	Elbows		Wrists and Hands		Knees		Ankles and Feet	
	Tube A	Tube B	Tube A	Tube B	Tube A	Tube B	Tube A	Tube B
Effective $CTDI_w$	8.7442	8.7442	10.2119	10.2119	11.503	11.503	11.503	11.503
Effective tube current–time product (mAs)	202	101	236	118	248	124	248	124
Pitch factor	0.70	0.70	0.70	0.70	0.70	0.70	0.70	0.70
Quality reference tube current–time product (mAs)	202	101	202	101	249	124	249	124
Rotation time (s)	0.330	0.330	0.330	0.330	1.000	1.000	1.000	1.000
Slice width, collimated (mm)	0.60	0.60	0.60	0.60	0.60	0.60	0.60	0.60
Tube voltage (kV)	80	140	80	140	80	140	80	140

Note—$CTDI_w$ = weighted CT dose index.

TABLE 2: Incidences and Types of Artifact Identified on Dual-Energy CT

Artifact	Patients (n = 50)	
	No.	%
Nail bed	44	88
Skin	22	44
Submillimeter	14	28
Beam hardening	8	16
Other	6	12

TABLE 3: Incidences and Distribution of Skin and Nail Bed Artifacts on Dual-Energy CT

Artifact	Extremities		Patients	
	No.	%	No.	%
Skin				
Hand	4/90	4.4	2/46	4.3
Foot	36/100	36	21/50	42
Nail bed				
Hand	3/90	3.3	2/46	4.3
Foot	76/100	76	44/50	88

es of the hands and wrists, elbows, knees, and feet and ankles. The protocol settings are outlined in Table 1. Figure 1 shows the typical FOVs acquired during reformatting.

These studies are acquired using a DECT scanner (Somatom Definition [a dual-source 128-MDCT scanner], Siemens Healthcare). Data are simultaneously acquired at 80 and 140 kV and are then processed on a multimodality workstation (Syngo, Siemens Healthcare) with software (Syngo VE50A, Siemens Healthcare) using a two-material decomposition algorithm. The software color-codes monosodium urate as green, cortical bone as blue, and trabecular bone as pink and then fuses these color codes findings onto the standard gray-scale CT images. Images are displayed in axial, sagittal, coronal, and 3D reconstructions.

Fifty consecutive patients who underwent imaging with the DECT gout protocol over an 8.5-month period (January 26 to October 9, 2012) were identified retrospectively using an electronic search of our institution's in-house report database for the keywords "dual energy" and "gout." The inclusion criteria were that patients had undergone a full DECT gout protocol with the indication of suspected gout. Patients were excluded if they underwent only part of the gout protocol or if they were scanned for primary indications other than gout. Three patients were excluded because of a technical failure that prevented review of any of the gout protocol image series. Several individual study parts could not be reviewed because of loss of dual-energy data on the system: two pairs of elbows, two pairs of knees, four pairs of hands, and two left hands. In addition, two pairs of elbows were not imaged because of technical difficulties at the time of scanning. Therefore, DECT examinations of a total of 44 pairs of hands and wrists, two right hands and right wrists, 46 elbows, 48 knees, and 50 feet and ankles were reviewed.

Each case was double-read by two musculoskeletal radiologists with 7 and 30 years' experience who had undergone identical training to identify artifacts on DECT of patients with suspected gout. For two cases in which a discrepancy existed, agreement was reached by consensus. Ultimately, there was therefore no variation between the observers.

Artifacts were defined by the criteria listed in Appendix 1; these criteria are based on the observations of this study and others [8, 10, 11].

Results

Twenty-eight (56%) cases were positive for gout. Forty-five (90%) of the cases showed some form of artifact. The types and incidences of each artifact are summarized in Table 2.

The distribution of the skin and nail bed artifacts between the upper and lower limbs is shown in Table 3. It is noteworthy that no skin artifact was identified in the elbows or knees.

Submillimeter specks, most likely due to noise, were found exclusively in the soft tissues rather than bone. Typically submillimeter artifact was within the muscular compartments, but it was seen in a blood vessel in one case and in a knee meniscus in another case.

Beam-hardening artifact was caused by a source outside the scanned area in two cases; by jewelry (rings) in three cases; and by a radial buttress plate, a total knee replacement, and a surgical staple in once case each, respectively.

The "other" artifacts were associated with calcified vessels in four cases, bone cortex in one case, and motion artifact in one case.

Discussion

Artifact Types

Nail bed artifact—The most commonly encountered artifact was in the nails and nail beds of the feet and was seen in the majority of cases (76.0% of feet and 88.0% of patients) (Fig. 2). However, it was less common in the hand (3.3% of feet, 4.3% of patients).

TABLE 4: Artifact-Reduction Methods by Artifact Type

Artifact Type	Artifact-Reduction Methods
Motion	• Use tape or blocks to immobilize the patient's limbs • Increase the speed of the gantry from 1 rotation per second to 1 rotation every 0.3 s
Single pixel	• Use D24 kernel or Q34 kernel (iterative reconstruction) • Increase Range parameter from 3 to 5
Beam-hardening and metal	• Use D24, D34, or Q34 kernel to reconstruct • Remove metal (e.g., jewelry) where possible
Nail bed, skin, plantar fascia	• Increase Air Distance parameter from 5 to 10 • Decrease Bone Distance parameter from 10 to 5 • Use D33 kernel to reduce skin artifact
Vascular	• Increase Minimum and Range parameters • Add a new reconstruction with a softer kernel (D20 or D24) or add iterative reconstruction (e.g., Q30)

This artifact may be due to a similarity in the dual-energy index values—that is, the value calculated from attenuation change with energy level—of the keratinous nail bed and of monosodium urate.

Skin artifact—Skin artifact was also prevalent in the feet (36% of feet and 42% of patients) but, again, was less common in the hand (4.4% of hands and 4.3% of patients) (Fig. 3). No skin artifact was seen at the knees or elbows. The prevalence of skin artifact in the feet may relate to a relatively larger amount of thickened and callused skin in the feet. This theory is supported by the occurrence of artifact where two cutaneous surfaces are opposed—for example, between the digits or heels. Although tophaceous gout deposits are known to affect the skin, their morphology is typically that of nodular chalky masses, not a thin, even layer following the skin, as was observed in this study.

Submillimeter artifacts—Submillimeter artifacts may be single or may form part of a diffuse pattern of the scatter (Fig. 4). They are thought to occur as a result of and as a form of noise. However, if multiple tiny foci are seen in an anatomic distribution, such as along a tendon, then true deposition should be considered.

Anecdotally, we noted that when thin-slice data were processed using the urate algorithm, a uniformly green, finely pixelated pattern occurred diffusely throughout the skin of the hands, supporting the theory of a link between noise and gout artifact.

Beam hardening—Observations from this study show beam-hardening artifact is common where beam hardening is present, either from inside or outside the scanned image (Fig. 5). This artifact follows the path of the hardened beam and is confined to it. This phenomenon was seen within cortical bone of the radial head in one case. The fact that this isolated linear pattern was confined to the cortex in this case made intraarticular or intraosseous gout unlikely.

A single case from this study shows that artifact may be associated with motion. The key factor in interpreting this finding as artifact was the distribution through and restricted to a nonanatomic plane that corresponded to the blurred artifact plane on standard CT (Fig. 6).

An interesting "artifact" was noted within calcified vessels in four cases (Fig. 7). Three of the four cases showed a convincing urate deposition elsewhere in the lower limb, but the sample size is too small for a meaningful statistical correlation. A recent review suggested that urate may play a role in vascular endothelial dysfunction [12]. Frank cardiovascular urate deposits have been reported in the coronary and intraabdominal arteries, but not widely, and a review of 11 necropsied cases failed to show any urate in the peripheral vessels [13]. It is thought that noise within small structures may contribute to vascular artifact.

The high prevalence of artifact in DECT of suspected gout would make false-positives a common problem in the absence of their recognition. It is likely that there are times when artifacts are indistinguishable from true gout signals; this possibility would account for the results of previous studies showing DECT has less than 100% specificity for gout. It would seem logical that because urate deposition is a continuous, not discrete, process, some submillimeter deposits could represent tiny deposits of true gout. Gouty tophi can be found within the skin and therefore so potentially could true gout signals. If beam hardening was not well identified—for example, if the artifact was diffuse or the study was noisy, then the resulting artifact could be misinterpreted. However, we believe that in most cases, artifacts in the DECT gout protocol are readily recognizable, allowing a high specificity for gout when the reporting radiologist is aware of these potential artifacts.

Artifact-Reduction Techniques

Reduction of artifacts in dual-energy scanning can be achieved in several ways (Table 4): physical adjustments of the patient at the time of scanning, adjustment of gantry speed, the use of kernels, and adjustment of settings at the workstation using the advanced parameter definition table.

Kernels—Different kernels (i.e., specialized reconstruction algorithms) can be used to optimize the views of the anatomic structure of interest. Kernels act as filters that can smooth the image and reduce or eliminate beam-hardening artifacts. On the Siemens system we used for this study, Q algorithms use iterative reconstruction to achieve noise reduction and also eliminate beam-hardening artifacts. D kernels use filtered back projection. D34F is a specific kernel to reduce beam hardening from bone. Q kernels are probably superior to D kernels, although no formal comparison has yet been made in clinical studies to our knowledge.

Parameters—Adjustments can be made to the image by the radiologist at the time of interpretation using the DECT software advanced parameter definition table (Fig. 8). The optimal settings have been determined by in vivo and in vitro studies and are preset by the manufacturer; however, small adjustments by the radiologist can help reduce artifact in some situations as defined in Table 4.

The graph in the advanced parameter definition table (Fig. 8) is a plot of the attenuation of each voxel at 80 kV (*y*-axis) against the attenuation of each voxel at 140 kV (*x*-axis). The two-material decomposition algorithm separates the calcium and urate based on the different change in attenuation of each substance between the two energy levels, which is inde-

pendent of the density of the tissue. The blue baseline line divides calcium (trabecular bone and cortical bone), which lies above the line, from monosodium urate, which falls below the line. Soft tissue acts as the baseline.

The Soft Tissue setting (Fig. 8) refers to density and represents the apparent attenuation of soft tissue at the two energy levels used by the machine. We recommend using the preset value of 50 HU.

The Ratio setting (Fig. 8) adjusts the weighting between the two energy levels used to create the image and adjusts the slope of the graph. This setting alters differentiation between uric acid and calcium (cortical bone and trabecular bone). Adjustments to ratio improve sensitivity at the expense of specificity and vice versa. Increasing the ratio increases sensitivity, and decreasing improves specificity.

The Range setting (Fig. 8) adjusts the smoothness of the image at the expense of edge enhancement. Increasing the range will result in a smoother but less edge-enhanced picture and can thus improve artifact based on noise.

The Minimum and Maximum settings (Fig. 8) define the range over which the dual-energy index calculation occurs. Adjustments can reduce vascular artifact (Table 4).

The Air Distance and Bone Distance settings (Fig. 8) represent the minimum distance between the urate and the air and bone in units of voxels. Small adjustments can reduce skin and nail bed artifacts (Table 4).

Conclusion

Artifacts, although common in DECT gout protocol, can usually be readily recognized, thereby avoiding false-positive results. Knowledge of these artifacts is essential for the radiologist to accurately report studies performed with this powerful new imaging modality.

References

1. Kim KY, Ralph SH, Hunsche E, Wertheimer AI, Kong SX. A literature review of the epidemiology and treatment of acute gout. *Clin Ther* 2003; 25:1593–1617
2. So A, Busso N. Update on gout 2012. *Joint Bone Spine* 2012; 79:539–543
3. Pascual E, Batlle-Gualda E, Martínez A, Rosas J, Vela P. Synovial fluid analysis for diagnosis of intercritical gout. *Ann Intern Med* 1999; 131:756–759
4. Monu JU, Pope TL Jr. Gout: a clinical and radiologic review. *Radiol Clin North Am* 2004; 42:169–184
5. Nicolaou S, Yong-Hing CJ, Galea-Soler S, Hou DJ, Louis L, Munk P. Dual-energy CT as a potential new diagnostic tool in the management of gout in the acute setting. *AJR* 2010; 194:1072–1078
6. Graser A, Johnson TR, Bader M, et al. Dual energy CT characterization of urinary calculi: initial in vitro and clinical experience. *Invest Radiol* 2008; 43:112–119
7. Choi HK, Burns LC, Shojania K, et al. Dual energy CT in gout: a prospective validation study. *Ann Rheum Dis* 2012; 71:1466–1471
8. Glazebrook KN, Guimaraes LS, Murthy NS, et al. Identification of intraarticular and periarticular uric acid crystals with dual-energy CT: initial evaluation. *Radiology* 2011; 261:516–524
9. Nicolaou S. Dual energy CT in the detection of monosodium urate in patients with gouty arthropathy. (abstract) In: *Proceedings of the 96th scientific assembly and annual meeting of the Radiological Society of North America*. Oak Brook, IL: RSNA, 2010
10. Johnson TR, Fink C, Schonberg SO, Reiser MF. *Dual energy CT in clinical practice*, 1st ed. New York, NY: Springer-Verlag, 2011
11. Tashakkor AY, Wang JT, Tso D, Choi HK, Nicolaou S. Dual-energy computed tomography: a valid tool in the assessment of gout? *Int J Clin Rheumatol* 2012; 7:73–79
12. Edwards NL. The role of hyperuricemia and gout in kidney and cardiovascular disease. *Cleve Clin J Med* 2008; 75(suppl 5):S13–S16
13. Levin MH. Lichtenstein L, Scott HW. Pathologic changes in gout: survey of eleven necropsied cases. *Am J Pathol* 1956; 32:871–895

Fig. 1—Reformatted dual-energy CT (DECT) images of 63-year-old man with suspected gout shows typical scanning ranges for each body part imaged for gout protocol. Views show craniocaudal extent of scanning for each body part. FOV encompasses both limbs so they are viewed as pair.

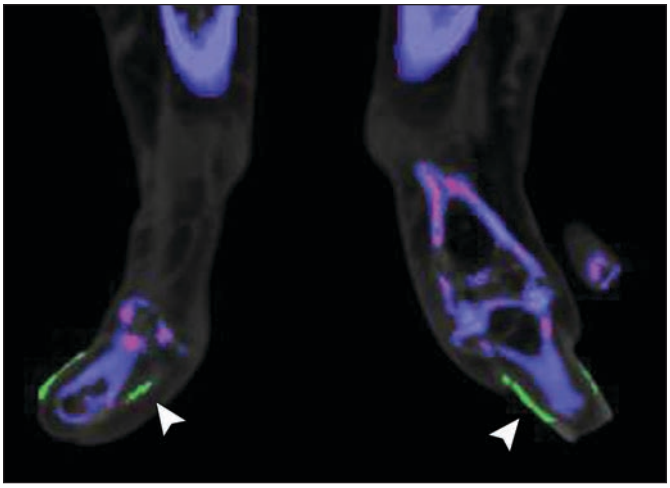

A

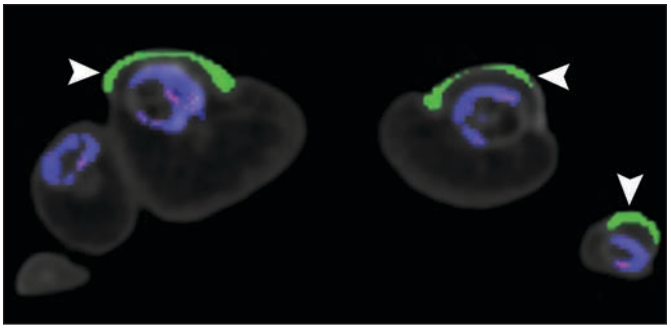

B

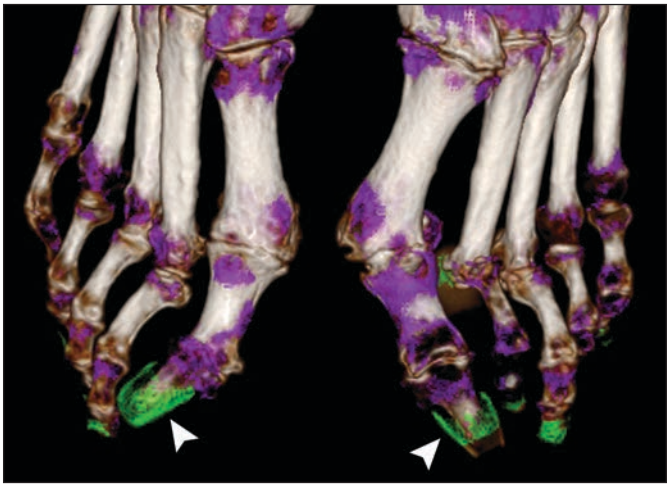

C

Fig. 2—Nail bed artifact on dual-energy CT (DECT) images of 65-year-old man with suspected gout.
A and **B,** Nail bed artifacts (*arrowheads*) are visible on axial DECT image.
C, Nail bed artifacts (*arrowheads*) are visible on 3D DECT reconstruction.

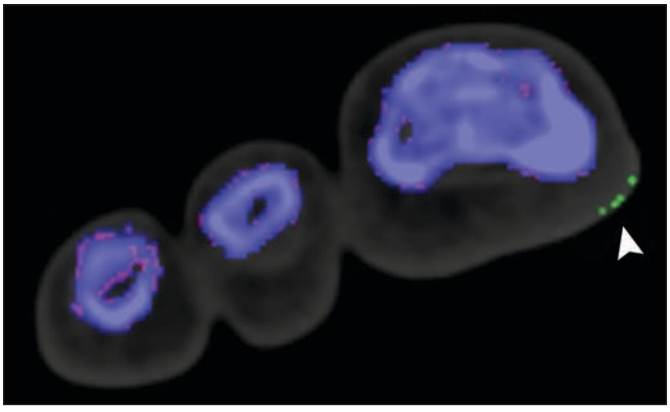

A

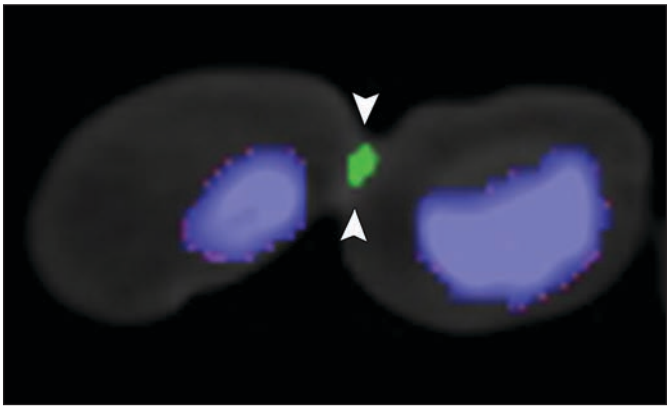

B

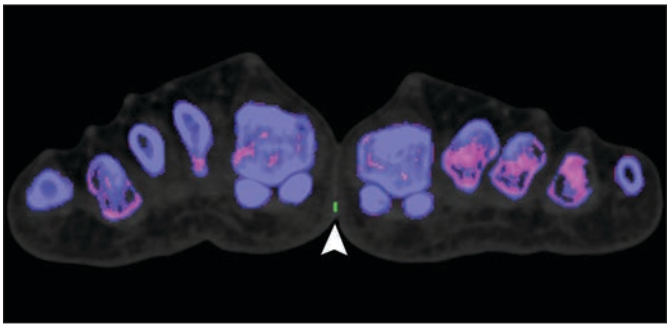

C

Fig. 3—Skin artifact on dual-energy CT (DECT) images of patients with suspected gout.
A, Skin artifact (*arrowhead*) is seen in hallux on coronal DECT image of 32-year-old man.
B, Skin artifact (*arrowheads*) is seen between two opposed toes on coronal DECT image of 74-year-old woman.
C, Skin artifact (*arrowhead*) is seen between two opposed feet on coronal DECT image of 66-year-old man.

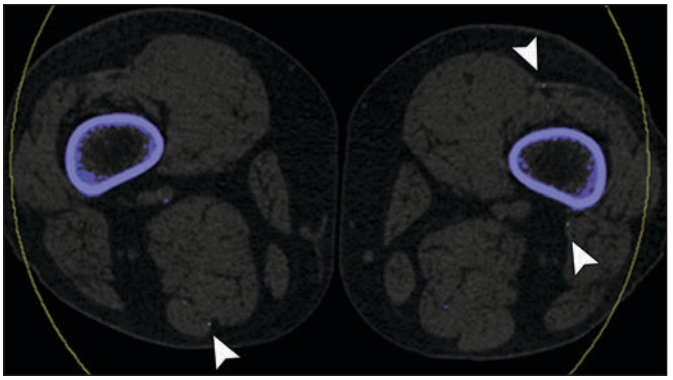

Fig. 4—Submillimeter artifact (*arrowheads*) is seen on axial dual-energy CT (DECT) image of thighs of 67-year-old woman.

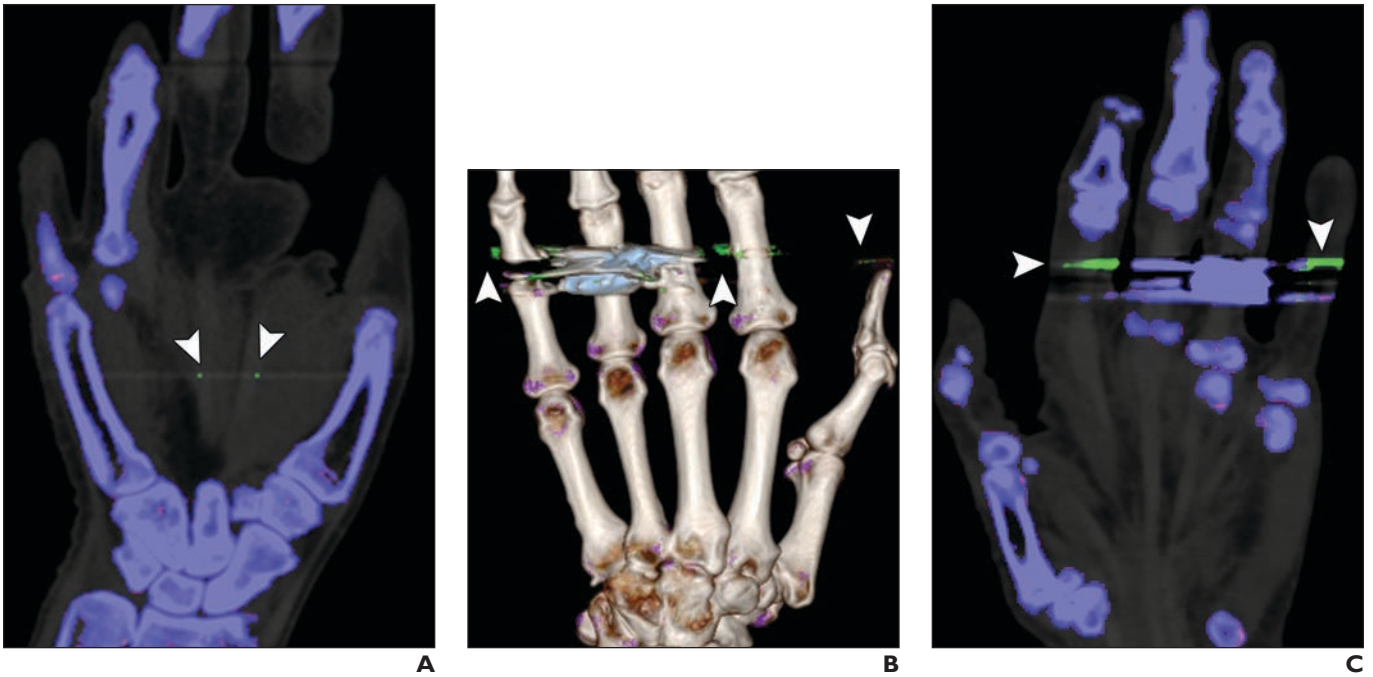

Fig. 5—Beam-hardening artifact on dual-energy CT (DECT) images of patients with suspected gout.
A, Beam-hardening artifact (*arrowheads*) from source outside scanned area is visible on coronal DECT image of 51-year-old man. All of artifact lies along hardened beam path.
B and **C,** Beam-hardening artifact (*arrowheads*) from jewelry (ring) on finger is seen on 3D (**B**) and coronal (**C**) DECT views of 68-year-old woman.

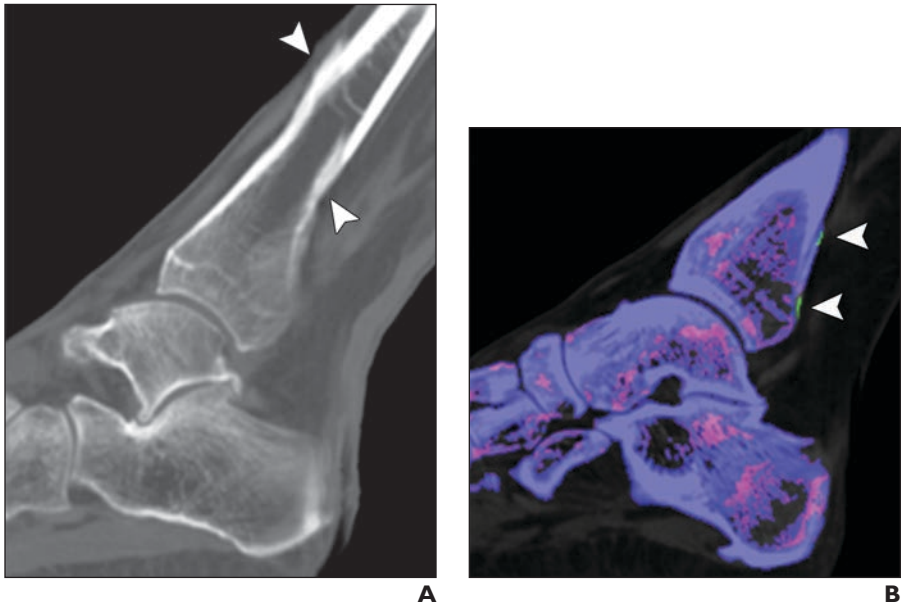

Fig. 6—Artifacts on dual-energy CT (DECT) images of 50-year-old man with suspected gout.
A, Artifact (*arrowheads*) secondary to motion is seen on standard sagittal CT image.
B, Associated green artifact (*arrowheads*) is visible on sagittal DECT image.

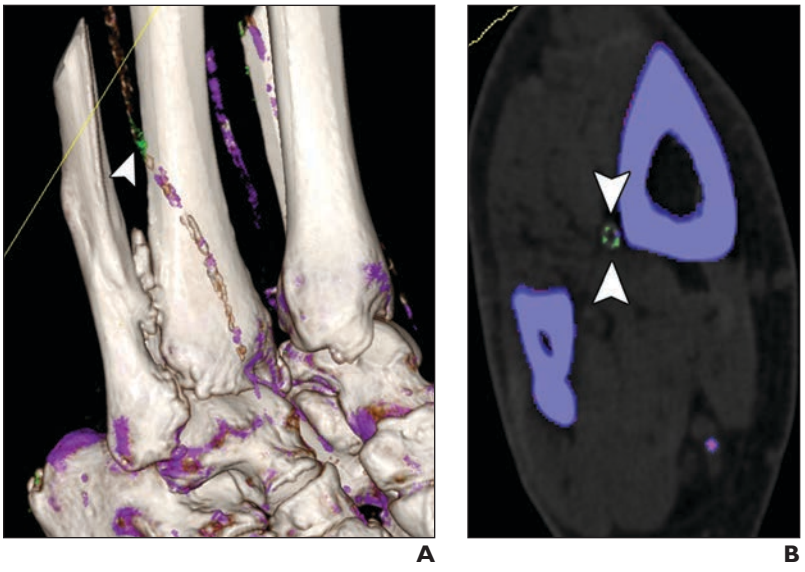

Fig. 7—Likely arterial artifacts on dual-energy CT (DECT) images of 67-year-old man with suspected gout.
A, Likely arterial artifact in calcified vessels (*arrowhead*) is seen on 3D DECT image.
B, Likely arterial artifact in calcified vessels (*arrowhead*) is visible on axial DECT image.

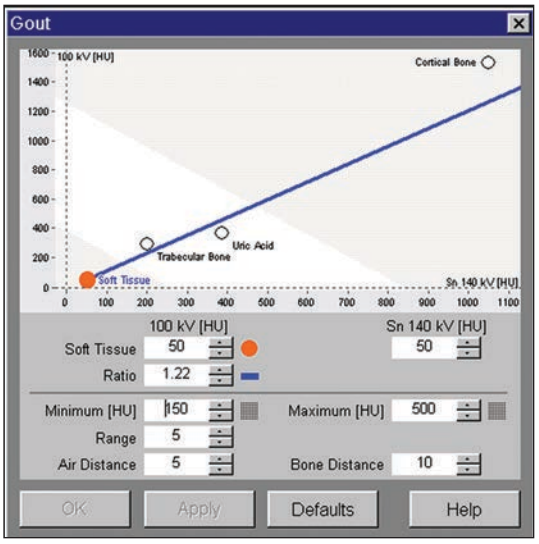

Fig. 8—Screen shot from dual-energy CT (DECT) software shows advanced parameter definition table. Optimal settings have been determined by in vivo and in vitro studies and are preset; however, small adjustments by radiologist can help reduce artifact in some situations. Graph is plot of attenuation of each voxel at 80 kV (*y*-axis) against attenuation of each voxel at 140 kV (*x*-axis). Two-material decomposition algorithm separates calcium and urate based on different change in attenuation of each substance between two energy levels, which is independent of density of tissue. Blue baseline line divides calcium (trabecular bone and cortical bone), which lies above line, from monosodium urate, which falls below line. Soft tissue acts as baseline.

APPENDIX 1: Artifacts in Dual-Energy CT (DECT) Gout Protocol Based on Observations From This Study and Others [8, 10, 11]

Artifacts in DECT Gout Protocol

- Green coloring of nails or nail beds that is confined to the nails or nail beds
- Green coloring of the skin that is confined to the skin
- Coloring of single pixels or areas smaller than 1 mm
- Coloring associated with beam-hardening artifact (confined to the plane of beam hardening) or motion artifact including artifact following and confined to areas of bone cortex
- Green coloring associated with calcified vessels